

Low-Complexity Receiver Design for Affine Filter Bank Modulation

Kuranage Roche Rayan Ranasinghe[†], Bruno S. Chang^{*,*} and Giuseppe Thadeu Freitas de Abreu[†]

[†]School of Computer Science and Engineering, Constructor University, Bremen, Germany

^{*}CPGEI/Electronics Department, Federal University of Technology - Paraná, Curitiba, Brazil

Abstract—We propose a low-complexity receiver structure for the recently introduced Affine Filter Bank Modulation (AFBM) scheme, which is a novel waveform designed for integrated sensing and communications (ISAC) systems operating in doubly-dispersive (DD) channels. The proposed receiver structure is based on the Gaussian Belief Propagation (GaBP) framework, making use of only element-wise scalar operations to perform detection of the transmitted symbols. Simulation results demonstrate that AFBM in conjunction with GaBP outperforms affine frequency division multiplexing (AFDM) in terms of bit error rates (BERs) in DD channels, while achieving very low out-of-band emissions (OOBE) in high-mobility scenarios.

Index Terms—Doubly-dispersive, ISAC, AFDM, AFBM.

I. INTRODUCTION

Wireless communications systems are increasingly required to support a wide range of applications such as high-mobility communications [1], computing functionalities [2], [3], and integrated sensing and communications (ISAC) [4]–[6]. The high mobility and/or frequencies associated with such applications, however, imply the presence of doubly-dispersive (DD) channels, which are known [7] to lead to severe inter-carrier interference and consequent link performance degradation of to orthogonal frequency division multiplexing (OFDM), the waveform used in most modern communications systems.

To overcome this challenge, several novel waveforms have been proposed in the last years [8], with affine frequency division multiplexing (AFDM) being one of the most recent and promising solutions. The AFDM [9] waveform maps data symbols into chirp-based subcarriers in the discrete affine Fourier (DAF) domain, and is capable of attaining full diversity in DD channels via the adjustment of chirp parameters, which are tuned based on the channel characteristics. However, AFDM suffers from a high peak-to-average power ratio (PAPR) and poor spectral containment, leading to challenges in implementation such as inefficient power amplification and high out-of-band emissions (OOBE).

Significant effort has been made recently, therefore, to address these limitations. In [10], for instance, an access scheme was proposed in which the discrete Fourier transform (DFT) operation of a spread-OFDM system (DFT-s-OFDMA) was replaced by a discrete affine Fourier transform (DAFT), yielding a spread-AFDM access (DAFT-s-AFDMA) approach shown to have improved PAPR properties. In turn, in [11] a modified version of orthogonal chirp division multiplexing (OCDM) dubbed c-OCDM was presented, where spectral containment is improved by applying zero-padding in the

frequency domain on the chirp matrices prior to modulation. And given that AFDM and OCDM differ mainly on the choice of chirp parameters, the spectral containment approach of [11], it is natural that a similar idea was presented for AFDM in [12], where a modified transceiver structure to reduce the overall computational complexity is also shown.

Approaching the problem from the perspective of OOBE, on the other hand, Filter Bank Multicarrier Modulation (FBMC) emerges as an alternative to design DD-robust ISAC waveforms, due to the per-subcarrier filtering process inherent of filter-bank methods. And while regular FBMC systems are limited to real orthogonality and offset quadrature amplitude modulation (OQAM) modulation to fulfill the Balian-Low theorem, precoded versions such as those proposed in [13]–[16] allow the restoration of complex orthogonality, with additional low PAPR features obtained via DFT-pruning.

Affine Filter Bank Modulation (AFBM), first proposed in [17], is a novel multicarrier waveform designed to enable ISAC in DD channels while maintaining the low PAPR and OOBE characteristics of typical filter bank-based multicarrier systems. However, the receiver design for AFBM has not been addressed yet, and the existing approaches for AFDM are not directly applicable due to the additional complexity introduced by the chirp-based subcarriers and the filtering process. In this paper, we propose a low-complexity receiver structure for AFBM based on the Gaussian Belief Propagation (GaBP) framework, which is capable of performing detection of the transmitted symbols using only element-wise scalar operations, as demonstrated via simulation results.

II. SIGNAL MODEL

Consider a point-to-point communication system with a single-antenna transmitter (TX) and receiver (RX) operating in a DD channel, using the proposed AFBM waveform. Following the typical filter bank-based multicarrier system structure, transmit symbols are mapped onto a grid with L subcarriers and K time indices. However, in order to maintain complex orthogonality, and since half of the system's L subcarriers must be reserved as a guard interval to avoid filter interference, transmission is carried out at a double rate with respect to the conventional transmission seen in OFDM/AFDM systems, namely, every $L/2$ samples (see [18] for more details on the oversampling effect tradeoff with AFDM).

The considered filter bank-based system can be characterized as a block structure composed of K symbols with a

duration of $T/2$ seconds, where each symbol has L subcarriers spaced by F Hz. Thus, in the TF domain we obtain a grid with L points spaced by F Hz along the frequency axis and K points along the time axis with a space of $T/2$ seconds. In this sense, the total bandwidth is defined as $B = LF$ and the total transmission time interval as $KT/2$.

A. Transmit Signal

Let $\mathbf{x} \in \mathcal{D}^{K \frac{L}{2} \times 1}$ denote the vector containing the transmit symbols, where \mathcal{D} denotes an arbitrary modulation alphabet of size $|\mathcal{D}|$, such as quadrature amplitude modulation (QAM).

The symbols in \mathbf{x} are organized via insertion in the first and last $L/4$ positions in a matrix $\mathbf{A} \in \mathbb{C}^{L \times K}$ according to a pre-established transmission strategy in order to avoid interference from the filter bank, given by the relationship

$$\mathbf{a} \triangleq \text{vec}(\mathbf{A}) = \mathbf{\Xi} \mathbf{x} \in \mathbb{C}^{LK \times 1}, \quad (1)$$

where $\text{vec}(\cdot)$ denotes the column-wise vectorization operation and $\mathbf{\Xi} \in \mathbb{C}^{LK \times K \frac{L}{2}}$ is constructed as

$$\mathbf{\Xi} \triangleq \mathbf{I}_K \otimes \mathbf{\bar{\Xi}}, \quad (2)$$

with $\mathbf{\bar{\Xi}} \in \mathbb{C}^{L \times \frac{L}{2}}$ defined as

$$\mathbf{\bar{\Xi}} \triangleq \begin{bmatrix} \mathbf{I}_{L/4} & \mathbf{0}_{L/4} \\ \mathbf{0}_{L/2} & \mathbf{0}_{L/2} \\ \mathbf{0}_{L/4} & \mathbf{I}_{L/4} \end{bmatrix}, \quad (3)$$

where $\mathbf{0}_L$ denotes a full zero matrix of size L .

Then, the vectorized form of the DAFT-spread transmit signal $\mathbf{b} \in \mathbb{C}^{LK \times 1}$ whose matrix form is defined as $\mathbf{B} \in \mathbb{C}^{L \times K}$ before the prototype filter is given by

$$\begin{aligned} \mathbf{b} \triangleq \text{vec}(\mathbf{B}) &= \text{vec}(\underbrace{\mathbf{W}_L \text{diag}(\tilde{\mathbf{b}})}_{\triangleq \mathbf{C}_f \in \mathbb{C}^{L \times L}} \mathbf{A}) = \underbrace{(\mathbf{I}_K \otimes \mathbf{C}_f)}_{\triangleq \mathbf{C} \in \mathbb{C}^{LK \times LK}} \text{vec}(\mathbf{A}) \\ &= \mathbf{C} \mathbf{a} = \mathbf{C} \mathbf{\Xi} \mathbf{x}. \end{aligned} \quad (4)$$

where $\mathbf{W}_L \in \mathbb{C}^{L \times L}$ represents the L -point DAFT matrix, *i.e.*

$$\mathbf{W}_L = \mathbf{\Lambda}_{c_1, L} \mathbf{F}_L \mathbf{\Lambda}_{c_2, L}, \quad (5)$$

with $\mathbf{\Lambda}_{c_i, L} = \text{diag}[e^{-j2\pi c_i(0)^2}, \dots, e^{-j2\pi c_i(L-1)^2}] \in \mathbb{C}^{L \times L}$ denoting an L -size diagonal chirp matrix with a central digital frequency of c_i , \mathbf{F}_L a normalized L -point DFT matrix and $\tilde{\mathbf{b}} \in \mathbb{C}^{L \times 1}$ the filter compensation vector.

We emphasize that $\tilde{\mathbf{b}}$ is needed for transceiver complex orthogonality, as detailed in [17, Eq.(12)]. From the above, the DAFT $\tilde{\mathbf{W}}_P \in \mathbb{C}^{L \times P}$ can be expressed as

$$\tilde{\mathbf{W}}_P = [\mathbf{I}_L \quad \mathbf{0}_{L \times (P-L)}] \mathbf{W}_P. \quad (6)$$

Afterwards, by using frequency domain zero padding, the output matrix \mathbf{Q}_P for a given block can be generated as

$$\mathbf{Q}_P = \mathbf{F}_N^H \mathbf{T} \mathbf{F}_P \tilde{\mathbf{W}}_P^H, \quad (7)$$

where $\mathbf{T} \triangleq [\mathbf{I}_{P,l}^T \quad \mathbf{0}_{(N-P) \times P} \quad \mathbf{I}_{P,u}^T]$, with $\mathbf{T}^T \mathbf{T} = \mathbf{I}_P$, is an $N \times P$ matrix, with $\mathbf{I}_{P,u}$ and $\mathbf{I}_{P,l}$ denoting the first and last $P/2$ columns of the $P \times P$ identity matrix \mathbf{I}_P , respectively.

Considering the transmission of K blocks, the block matrix $\mathbf{Q} \in \mathbb{C}^{NK \times LK}$ is defined as

$$\mathbf{Q} = \mathbf{I}_K \otimes \mathbf{Q}_P, \quad (8)$$

where \otimes refers to the Kronecker product which maps \mathbf{Q}_P to the correct time positions.

Then, the transmitted data can be obtained by convolving the output with the prototype filter impulse response through a Toeplitz filter matrix. Let us consider the diagonal matrix \mathbf{G}_p corresponding to the filter coefficients, that is, $\mathbf{G}_p = \text{diag}(\mathbf{g}_p) \in \mathbb{R}^{N/2 \times N/2}$ for $p = 0, 1, 2, \dots, 2O - 1$, where \mathbf{g}_p is given by $\mathbf{g}_p = [g[pN/2], g[pN/2+1], \dots, g[pN/2+N/2-1]]$ and \mathbf{g} is the prototype filter of length ON , where O is the filter overlap factor. Thus, the block Toeplitz filter matrix $\mathbf{G} \in \mathbb{R}^{ON+(K-1)N/2 \times NK}$ can be generated from the vector $[\mathbf{G}_0 \mathbf{G}_1 \mathbf{G}_2 \dots \mathbf{G}_{2O-1}]^T$, as detailed in [17, Eq.(7)].

Then, the full AFBM transmit signal in the time-domain (TD) can be efficiently described in terms of the filter matrix \mathbf{G} , modified inverse discrete affine Fourier transform (IDAFIT) matrix \mathbf{Q}_P , and the compensation matrix \mathbf{C}_f leveraging identities involving Kronecker products as

$$\begin{aligned} \mathbf{s} &= \mathbf{G} \mathbf{Q} \mathbf{C} \mathbf{a} = \mathbf{G} (\mathbf{I}_K \otimes \mathbf{Q}_P) \cdot (\mathbf{I}_K \otimes \mathbf{C}_f) \mathbf{a} \in \mathbb{C}^{M \times 1} \\ &= \mathbf{G} (\mathbf{I}_K \otimes \mathbf{Q}_P \mathbf{C}_f) \mathbf{\Xi} \mathbf{x}, \end{aligned} \quad (9)$$

where $M \triangleq ON + \frac{N}{2}(K-1)$, and the symbols are delayed from each other every $N/2$ samples, as clarified by the blocks $\mathbf{0}_{N/2}$ in \mathbf{G} [16].

From the above, the proposed structure is an affine-precoded filter bank scheme can be implemented efficiently using a polyphase network (PPN) together with an inverse fast Fourier transform (IFFT). Another interpretation is that in the proposed waveform the standard AFDM sinc chirp subcarriers were replaced with chirp filtered ones. In addition, the length P of the IDAFIT at the transmitter must be greater than L to prevent the precoding stage DAFT from being nullified by the IDAFIT of the filter bank structure. Finally, P must be smaller than the size of the filter bank N so that the chirps are sampled at a rate lower than Nyquist's, allowing frequency containment.

B. Received Signal

The signal vector \mathbf{s} defined in equation (9) is transmitted over a time-varying multipath channel, *i.e.*, the doubly-dispersive channel, described concisely by the circular convolutional matrix form $\mathbf{H} \in \mathbb{C}^{M \times M}$ [14]. Consequently, the received signal $\mathbf{r} \in \mathbb{C}^{M \times 1}$ is expressed as

$$\mathbf{r} \triangleq \left(\sum_{r=1}^R h_r \Phi_r \mathbf{Z}^{f_r} \mathbf{\Pi}^{\ell_r} \right) \mathbf{G} (\mathbf{I}_K \otimes \mathbf{Q}_P \mathbf{C}_f) \mathbf{\Xi} \mathbf{x} + \mathbf{n}, \quad (10)$$

where $\mathbf{n} \in \mathbb{C}^{M \times 1}$ represents additive white Gaussian noise (AWGN) samples with zero mean and power σ_n^2 , while $\mathbf{H} \triangleq \sum_{r=1}^R h_r \Phi_r \mathbf{Z}^{f_r} \mathbf{\Pi}^{\ell_r} \in \mathbb{C}^{M \times M}$, parametrized by the complex channel fading coefficient $h_r \in \mathbb{C}$, is the doubly-dispersive wireless channel described by R resolvable propagation paths, and it is implicitly assumed that each r -th scattering path induces a delay $\tau_r \in [0, \tau^{\max}]$ and Doppler shift $\nu_r \in [-\nu^{\max}, +\nu^{\max}]$ to the received signal, where $\ell_r \triangleq \lfloor \frac{\tau_r}{T_s} \rfloor \in \mathbb{N}_0$ and $f_r \triangleq \frac{N\nu_r}{f_s} \in \mathbb{R}$ are the corresponding normalized integer path delay and normalized digital Doppler shift, with sampling frequency $f_s \triangleq \frac{1}{T_s}$.

As elaborated in [8], each r -th path of the full circular convolutional matrix \mathbf{H} , is parametrized by the complex channel fading coefficient $h_r \in \mathbb{C}$, the diagonal prefix phase

matrix $\Phi_r \in \mathbb{C}^{M \times M}$ with the IDAFT-based chirp-cyclic prefix phase function $\phi(m) \triangleq c_1(M^2 - 2Mm)$, given by

$$\Phi_r \triangleq \text{diag}[e^{-j2\pi \cdot \phi(\ell_r)}, \dots, e^{-j2\pi \cdot \phi(1)}, 1, \dots, 1] \in \mathbb{C}^{M \times M}, \quad (11)$$

the diagonal roots-of-unity matrix $\mathbf{Z} \in \mathbb{C}^{M \times M}$ given by

$$\mathbf{Z} \triangleq \text{diag}[e^{-j2\pi \frac{0}{M}}, \dots, e^{-j2\pi \frac{M-1}{M}}] \in \mathbb{C}^{M \times M}, \quad (12)$$

which is taken to the f_r -th power, and the right-multiplying circular left-shift matrix $\mathbf{\Pi} \in \mathbb{C}^{M \times M}$.

Next, the received signal is demodulated by $(\mathbf{G}\mathbf{Q})^H$, generating $\tilde{\mathbf{a}} \in \mathbb{C}^{LK \times 1}$. Then (and considering all time instants), the detected symbols represented by $\tilde{\mathbf{B}} \in \mathbb{C}^{L \times K}$ are obtained through the IDAFT combined with the compensation stage

$$\tilde{\mathbf{B}} = \mathbf{W}_L^H \text{diag}\{\tilde{\mathbf{b}}\} \tilde{\mathbf{A}}, \quad (13)$$

where $\tilde{\mathbf{A}} = [\tilde{\mathbf{a}}_0; \tilde{\mathbf{a}}_1; \dots; \tilde{\mathbf{a}}_{K-1}] \in \mathbb{C}^{L \times K}$.

To obtain the estimated symbols, the $L/2$ intermediate values between the first and last $L/4$ symbols are discarded, since no data is at those positions in \mathbf{A} . For symmetry reasons, the compensation stage is used in both the receiver and transmitter, which can be applied only to one side effectively.

Concatenating all these effects, the final received signal $\mathbf{y} \in \mathbb{C}^{K \frac{L}{2} \times 1}$ after demodulation without noise can be expressed as

$$\mathbf{y} \triangleq \Xi^H (\mathbf{I}_K \otimes \mathbf{C}_f^H \mathbf{Q}_P^H) \mathbf{G}^H \mathbf{H} \mathbf{G} (\mathbf{I}_K \otimes \mathbf{Q}_P \mathbf{C}_f) \Xi \mathbf{x}, \quad (14)$$

such that an end-to-end effective channel matrix can be extracted, which is given by

$$\mathbf{H}_{\text{eff}} \triangleq \Xi^H (\mathbf{I}_K \otimes \mathbf{C}_f^H \mathbf{Q}_P^H) \overbrace{\mathbf{G}^H \mathbf{H} \mathbf{G} (\mathbf{I}_K \otimes \mathbf{Q}_P \mathbf{C}_f)}^{\mathbf{H} \in \mathbb{C}^{NK \times K \frac{L}{2}}} \Xi. \quad (15)$$

III. PROPOSED GABP-BASED RECEIVER DESIGN

From a receiver design viewpoint, we aim to estimate the transmit signal \mathbf{x} , under the assumption that the filtered TD channel matrix $\tilde{\mathbf{H}} \in \mathbb{C}^{NK \times K \frac{L}{2}}$ is known¹, such that in order to derive a GaBP-based detector for the AFBM waveforms, we consider the I/O relationship given by

$$\tilde{\mathbf{r}} = \tilde{\mathbf{H}}\mathbf{x} + \tilde{\mathbf{w}}. \quad (16)$$

For comparison, the equivalent high-complexity linear minimum mean square error (LMMSE) can be expressed as

$$\hat{\mathbf{x}}_{\text{LMMSE}} = (\tilde{\mathbf{H}}^H \tilde{\mathbf{H}} + \sigma_n^2 \mathbf{I}_M)^{-1} \tilde{\mathbf{H}}^H \tilde{\mathbf{r}}. \quad (17)$$

Note that as a consequence of this approach, no additional demodulation stage is required after the effects of \mathbf{G} are reversed for data detection.

Setting $\bar{N} \triangleq NK$ and $\bar{M} \triangleq K \frac{L}{2}$ with $\bar{n} \triangleq \{1, \dots, \bar{N}\}$ and $\bar{m} \triangleq \{1, \dots, \bar{M}\}$, the element-wise relationship corresponding to equation (16) is given by

$$\tilde{r}_{\bar{n}} = \sum_{\bar{m}=1}^{\bar{M}} \tilde{h}_{\bar{n}, \bar{m}} x_{\bar{m}} + \tilde{w}_{\bar{n}}, \quad (18)$$

such that the soft replica of the \bar{m} -th communication symbol associated with the \bar{n} -th receive signal $\tilde{r}_{\bar{n}}$, computed at the i -th iteration of a message-passing algorithm can be denoted by $\hat{x}_{\bar{n}, \bar{m}}^{(i)}$, with the corresponding mean-squared-error (MSE) of these estimates computed for the i -th iteration given by

¹The final input-output (I/O) relationship portrayed in equation (14) is not used since the Gram matrix of \mathbf{H}_{eff} does not approach a clear diagonal.

$$\hat{\sigma}_{x:\bar{n}, \bar{m}}^{2(i)} \triangleq \mathbb{E}_x [|x - \hat{x}_{\bar{n}, \bar{m}}^{(i-1)}|^2] = E_S - |\hat{x}_{\bar{n}, \bar{m}}^{(i-1)}|^2, \forall (\bar{n}, \bar{m}), \quad (19)$$

where \mathbb{E}_x denotes expectation over all possible symbols x .

The GaBP receiver for such a setup consists of three major stages described below.

1) *Soft Interference Cancellation*: At a given i -th iteration of the soft interference cancellation (soft IC) stage of the algorithm, the soft replicas $\hat{x}_{\bar{n}, \bar{m}}^{(i-1)}$ from a previous iteration are used to calculate the data-centric soft IC signals $\tilde{r}_{x:\bar{n}, \bar{m}}^{(i)}$.

Exploiting equation (18), the soft IC signals are given by

$$\tilde{r}_{x:\bar{n}, \bar{m}}^{(i)} = \tilde{r}_{\bar{n}} - \sum_{e \neq \bar{m}} h_{\bar{n}, e} \hat{x}_{\bar{n}, e}^{(i)} = h_{\bar{n}, \bar{m}} x_{\bar{m}} + \overbrace{\sum_{e \neq \bar{m}} h_{\bar{n}, e} (x_e - \hat{x}_{\bar{n}, e}^{(i)})}^{\text{interference + noise term}} + \tilde{w}_{\bar{n}},$$

Using the scalar Gaussian approximation (SGA), the interference and noise terms highlighted above can be approximated as Gaussian noise, such that the conditional probability density functions (PDFs) of the soft IC signals become

$$p_{\tilde{r}_{x:\bar{n}, \bar{m}}^{(i)} | x_{\bar{m}}}(\tilde{r}_{x:\bar{n}, \bar{m}}^{(i)} | x_{\bar{m}}) \propto \exp \left[- \frac{|\tilde{r}_{x:\bar{n}, \bar{m}}^{(i)} - h_{\bar{n}, \bar{m}} x_{\bar{m}}|^2}{\hat{\sigma}_{x:\bar{n}, \bar{m}}^{2(i)}} \right], \quad (20)$$

with their conditional variances expressed as

$$\hat{\sigma}_{x:\bar{n}, \bar{m}}^{2(i)} = \sum_{e \neq \bar{m}} |h_{\bar{n}, e}|^2 \hat{\sigma}_{x:\bar{n}, e}^{2(i)} + \sigma_n^2. \quad (21)$$

2) *Belief Generation*: In the belief generation stage of the algorithm the SGA is exploited under the assumptions that \bar{N} is a sufficiently large number, and that the individual estimation errors in $\hat{x}_{\bar{n}, \bar{m}}^{(i-1)}$ are independent, in order to generate initial estimates (aka beliefs) for all the data symbols.

As a consequence of the SGA and with the conditional PDFs of equation (20), the following extrinsic PDFs

$$\prod_{e \neq \bar{n}} p_{\tilde{r}_{x:e, \bar{m}}^{(i)} | x_{\bar{m}}}(\tilde{r}_{x:e, \bar{m}}^{(i)} | x_{\bar{m}}) \propto \exp \left[- \frac{(x_{\bar{m}} - \bar{x}_{\bar{n}, \bar{m}}^{(i)})^2}{\bar{\sigma}_{x:\bar{n}, \bar{m}}^{2(i)}} \right], \quad (22)$$

are obtained, where the corresponding extrinsic means and variances are respectively defined as

$$\bar{x}_{\bar{n}, \bar{m}}^{(i)} = \bar{\sigma}_{x:\bar{n}, \bar{m}}^{(i)} \sum_{e \neq \bar{n}} \frac{h_{e, \bar{m}}^* \tilde{r}_{x:e, \bar{m}}^{(i)}}{\bar{\sigma}_{x:e, \bar{m}}^{2(i)}} \quad \text{and} \quad \bar{\sigma}_{x:\bar{n}, \bar{m}}^{2(i)} = \left(\sum_{e \neq \bar{n}} \frac{|h_{e, \bar{m}}|^2}{\bar{\sigma}_{x:e, \bar{m}}^{2(i)}} \right)^{-1}, \quad (23)$$

with $h_{e, \bar{m}}^*$ denoting the complex conjugate of $h_{e, \bar{m}}$.

3) *Soft Replica Generation*: Finally, the soft replica generation stage consists of denoising the previously computed beliefs under a Bayes-optimal rule, to obtain the final estimates for the desired variables. For quadrature phase-shift keying (QPSK) modulation², the Bayes-optimal denoiser is given by

$$\hat{x}_{\bar{n}, \bar{m}}^{(i)} = c_x \left(\tanh \left[2c_d \frac{\Re \bar{x}_{\bar{n}, \bar{m}}^{(i)}}{\bar{\sigma}_{x:\bar{n}, \bar{m}}^{2(i)}} \right] + j \tanh \left[2c_d \frac{\Im \bar{x}_{\bar{n}, \bar{m}}^{(i)}}{\bar{\sigma}_{x:\bar{n}, \bar{m}}^{2(i)}} \right] \right), \quad (24)$$

where $c_x \triangleq \sqrt{E_S/2}$ denotes the magnitude of the real and imaginary parts of the explicitly chosen QPSK symbols, with its corresponding variance updated as in equation (19).

²We consider QPSK for simplicity, but without loss of generality (wlg), since denoisers for other modulation schemes can also be designed [19].

After obtaining $\hat{x}_{\bar{n},\bar{m}}^{(i)}$ as per equation (24), the final outputs are computed by damping the results to prevent convergence to local minima due to incorrect hard-decision replicas [20]. Letting the damping factor be $0 < \beta_x < 1$ yields

$$\hat{x}_{\bar{n},\bar{m}}^{(i)} = \beta_x \hat{x}_{\bar{n},\bar{m}}^{(i)} + (1 - \beta_x) \hat{x}_{\bar{n},\bar{m}}^{(i-1)}. \quad (25a)$$

$$\hat{\sigma}_{x:\bar{n},\bar{m}}^{2(i)} = \beta_x (E_S - |\hat{x}_{\bar{n},\bar{m}}^{(i-1)}|^2) + (1 - \beta_x) \hat{\sigma}_{x:\bar{n},\bar{m}}^{2(i-1)}, \quad (25b)$$

Finally, as a result of the conflicting dimensions, the consensus update of the estimates can be obtained as

$$\hat{x}_{\bar{m}} = \left(\sum_{\bar{n}=1}^{\bar{N}} \frac{|h_{\bar{n},\bar{m}}|^2}{\hat{\sigma}_{x:\bar{n},\bar{m}}^{2(i_{\max})}} \right)^{-1} \left(\sum_{\bar{n}=1}^{\bar{N}} \frac{h_{\bar{n},\bar{m}}^* \hat{x}_{\bar{n},\bar{m}}^{(i_{\max})}}{\hat{\sigma}_{x:\bar{n},\bar{m}}^{2(i_{\max})}} \right). \quad (26)$$

IV. PERFORMANCE ANALYSIS

The complexity of the proposed GaBP detection algorithm is linear on the number of element-wise operations, and its per-iteration computational complexity is given by $\mathcal{O}(\bar{N}\bar{M})$. Notice that this complexity is much lesser than that of typical detection methods such as the LMMSE, which is $\mathcal{O}(\bar{M}^3)$ due to the costly matrix inversion involved.

For the simulations, the total number of subcarriers L is 128, the chirp size P is 256 and the filter bank DFT size N is 256. Each transmission was composed of $K = 8$ symbols, with a carrier frequency f_c of 4 GHz. The channel is a doubly dispersive one, with three resolvable paths and corresponding normalized delays and digital Doppler shifts. We recall that the chirp frequencies for each (1)DAFT were chosen to uphold the orthogonality condition [8] $2(f^{\max} + \xi)(\ell^{\max} + 1) + \ell^{\max} \leq P$, where f^{\max} and ℓ^{\max} are, respectively, the maximum normalized digital Doppler shift and delay of the channel and $\xi \in \mathbb{N}_0$ is a free parameter determining the so-called guard width, denoting the number of additional guard elements around the diagonals to anticipate for Doppler-domain interference.

Figures 1 and 2 presents bit error rate (BER) results from the considered systems. We remark that as opposed to the TD relationship in equation (16) considered for the proposed AFBM scheme, the typical DAF domain I/O presented in [6] is used for AFDM since the effective Gram matrix structures are almost identical. It can be seen that, the proposed GaBP-based AFBM scheme outperforms the regular AFDM scheme by approximately 2 dB at a BER of 10^{-3} , which is expected due to the better spectral localization and the reduced interference in the proposed scheme, even with varying P . Next, the OOBE and ambiguity functions of the considered schemes are shown in Figure 3. In this scenario, two prototype filters were considered for AFBM: the truncated Hermite (with $O = 1.5$) and the full PHYDYAS (with $O = 4$). Due to the usage of well-localized filters instead of the rectangular window there is a significant advantage in OOBE of the AFBM system with respect to regular AFDM. Finally, the ambiguity function of the AFBM system is also very similar that of the AFDM system, with a slightly better sidelobe suppression seen with the PHYDYAS prototype filter.

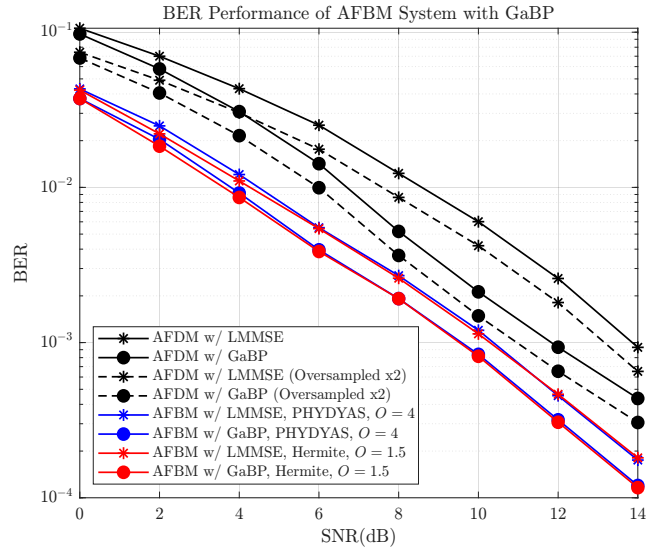


Fig. 1. BER performance of the proposed GaBP technique for both the AFDM and AFBM waveforms with Hermite and PHYDYAS prototype filters.

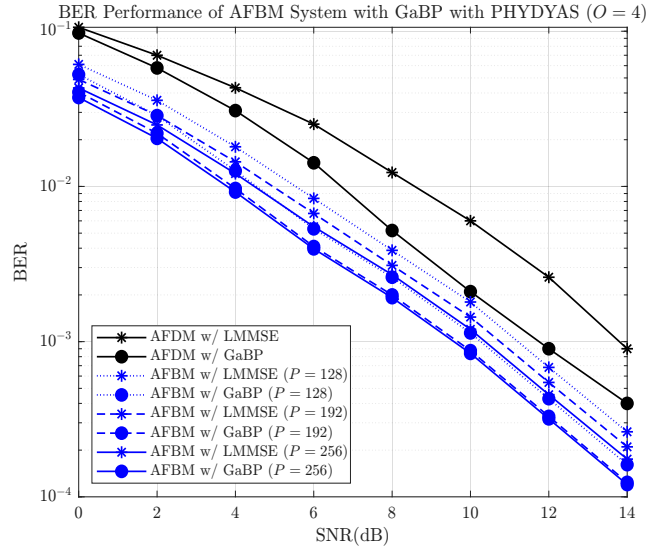


Fig. 2. BER performance of the proposed GaBP technique for both the AFDM and AFBM with PHYDYAS prototype filters for varying P .

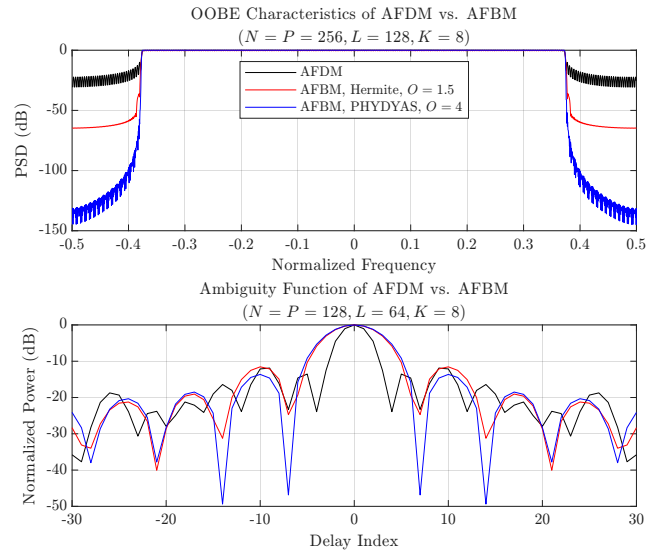


Fig. 3. OOBE and Ambiguity function Performance of AFDM and AFBM with the Hermite and PHYDYAS prototype filters.

REFERENCES

- [1] J. Wu and P. Fan, "A survey on high mobility wireless communications: Challenges, opportunities and solutions," *IEEE Access*, vol. 4, pp. 450–476, 2016.
- [2] K. R. Rayan Ranasinghe, K. Ando, and G. T. Freitas de Abreu, "From theory to reality: A design framework for integrated communication and computing receivers," in *2025 International Conference on Computing, Networking and Communications (ICNC)*, 2025, pp. 865–870.
- [3] K. R. R. Ranasinghe, K. Ando, H. S. Rou, G. T. F. de Abreu, T. Takahashi, M. D. Renzo, and D. G. G., "A flexible design framework for integrated communication and computing receivers," 2025. [Online]. Available: <https://arxiv.org/abs/2506.05944>
- [4] Z. Wei, H. Qu, Y. Wang, X. Yuan, H. Wu, Y. Du, K. Han, N. Zhang, and Z. Feng, "Integrated sensing and communication signals toward 5G-A and 6G: A survey," *IEEE Internet of Things Journal*, vol. 10, no. 13, pp. 11 068–11 092, 2023.
- [5] N. González-Prelcic, M. Furkan Keskin, O. Kaltiokallio, M. Valkama, D. Dardari, X. Shen, Y. Shen, M. Bayraktar, and H. Wymeersch, "The integrated sensing and communication revolution for 6G: Vision, techniques, and applications," *Proceedings of the IEEE*, vol. 112, no. 7, pp. 676–723, 2024.
- [6] K. R. R. Ranasinghe, H. Seok Rou, G. Thadeu Freitas de Abreu, T. Takahashi, and K. Ito, "Joint channel, data, and radar parameter estimation for afdm systems in doubly-dispersive channels," *IEEE Transactions on Wireless Communications*, vol. 24, no. 2, pp. 1602–1619, 2025.
- [7] J. Du and S. Signell, "Comparison of CP-OFDM and OFDM/OQAM in doubly dispersive channels," in *Future Generation Communication and Networking (FGCN 2007)*, vol. 2, 2007, pp. 207–211.
- [8] H. S. Rou, G. T. F. de Abreu, J. Choi, D. González G., M. Kountouris, Y. L. Guan, and O. Gonsa, "From orthogonal time–frequency space to affine frequency-division multiplexing: A comparative study of next-generation waveforms for integrated sensing and communications in doubly dispersive channels," *IEEE Signal Process. Mag.*, vol. 41, no. 5, pp. 71–86, 2024.
- [9] A. Bemani, N. Ksairi, and M. Kountouris, "Affine frequency division multiplexing for next generation wireless communications," *IEEE Transactions on Wireless Communications*, vol. 22, no. 11, pp. 8214–8229, 2023.
- [10] Y. Tao, M. Wen, Y. Ge, T. Mao, L. Xiao, and J. Li, "DAFT-spread affine frequency division multiple access for downlink transmission," in *GLOBECOM 2024 - 2024 IEEE Global Communications Conference*, 2024, pp. 2991–2996.
- [11] M. S. Omar and X. Ma, "Spectrum design for orthogonal chirp division multiplexing transmissions," *IEEE Wireless Communications Letters*, vol. 9, no. 11, pp. 1990–1994, 2020.
- [12] V. Savaux, "Special cases of DFT-based modulation and demodulation for affine frequency division multiplexing," *IEEE Transactions on Communications*, vol. 72, no. 12, pp. 7627–7638, 2024.
- [13] R. Zakaria and D. Le Ruyet, "A novel filter-bank multicarrier scheme to mitigate the intrinsic interference: Application to mimo systems," *IEEE Transactions on Wireless Communications*, vol. 11, no. 3, pp. 1112–1123, 2012.
- [14] R. Nissel and M. Rupp, "Pruned DFT-spread FBMC: Low PAPR, low latency, high spectral efficiency," *IEEE Transactions on Communications*, vol. 66, no. 10, pp. 4811–4825, 2018.
- [15] R. P. Junior, C. A. F. d. Rocha, B. S. Chang, and D. Le Ruyet, "A novel DFT precoded filter bank system with iterative equalization," *IEEE Wireless Communications Letters*, vol. 10, no. 3, pp. 478–482, 2021.
- [16] —, "A generalized DFT precoded filter bank system," *IEEE Wireless Communications Letters*, vol. 11, no. 6, pp. 1176–1180, 2022.
- [17] H. L. Senger, G. P. Gonçalves, B. S. Chang, H. S. Rou, K. R. R. Ranasinghe, G. T. F. de Abreu, and D. L. Ruyet, "Affine filter bank modulation: A new waveform for high mobility communications," 2025. [Online]. Available: <https://arxiv.org/abs/2505.03589>
- [18] K. R. Rayan Ranasinghe, Y. Ge, G. T. Freitas de Abreu, and Y. Liang Guan, "Joint channel estimation and data detection for afdm receivers with oversampling," in *2025 International Conference on Computing, Networking and Communications (ICNC)*, 2025, pp. 823–828.
- [19] T. Takahashi, S. Ibi, and S. Sampei, "Design of adaptively scaled belief in multi-dimensional signal detection for higher-order modulation," *IEEE Transactions on Communications*, vol. 67, no. 3, pp. 1986–2001, 2019.
- [20] Q. Su and Y.-C. Wu, "On convergence conditions of gaussian belief propagation," *IEEE Transactions on Signal Processing*, vol. 63, no. 5, pp. 1144–1155, 2015.